

OPTIMAL CONTROL OF HYBRID ELECTRIC VEHICLES

Master's thesis
performed in **Vehicular Systems**

by
Emma Strömberg

Reg nr: LiTH-ISY-EX-3394-2003

22nd August 2003

OPTIMAL CONTROL OF HYBRID ELECTRIC VEHICLES

Master's thesis

performed in **Vehicular Systems,**
Dept. of Electrical Engineering
at **Linköpings universitet**

by **Emma Strömberg**

Reg nr: LiTH-ISY-EX-3394-2003

Supervisor: **Ph.D. Student Anders Fröberg**
Linköpings Universitet

Examiner: **Professor Lars Nielsen**
Linköpings Universitet

Linköping, 22nd August 2003

	Avdelning, Institution Division, Department Vehicular Systems, Dept. of Electrical Engineering 581 83 Linköping	Datum Date 22nd August 2003
	Språk Language <input type="checkbox"/> Svenska/Swedish <input checked="" type="checkbox"/> Engelska/English <input type="checkbox"/> _____	Rapporttyp Report category <input type="checkbox"/> Licentiatavhandling <input checked="" type="checkbox"/> Examensarbete <input type="checkbox"/> C-uppsats <input type="checkbox"/> D-uppsats <input type="checkbox"/> Övrig rapport <input type="checkbox"/> _____
URL för elektronisk version http://www.vehicular.isy.liu.se http://www.ep.liu.se/exjobb/isy/2003/3394/		
Titel OPTIMAL STYRNING AV HYBRIDFORDON Title OPTIMAL CONTROL OF HYBRID ELECTRIC VEHICLES Författare Emma Strömberg Author		
Sammanfattning Abstract <p>Hybrid electric vehicles are considered to be an important part of the future vehicle industry, since they decrease fuel consumption without decreasing the performance compared to a conventional vehicle. They use two or more power sources to propel the vehicle, normally one combustion engine and one electric machine. These power sources can be arranged in different topologies and can cooperate in different ways. In this thesis, dynamic models of parallel and series hybrid powertrains are developed, and different strategies for how to control them are compared. An optimization algorithm for decreasing fuel consumption and utilize the battery storage capacity as much as possible is also developed, implemented and tested.</p>		
Nyckelord Keywords Hybrid Electric Vehicle, Modelling, Parallel HEV, Series HEV, Optimization, Prediction		

Abstract

Hybrid electric vehicles are considered to be an important part of the future vehicle industry, since they decrease fuel consumption without decreasing the performance compared to a conventional vehicle. They use two or more power sources to propel the vehicle, normally one combustion engine and one electric machine. These power sources can be arranged in different topologies and can cooperate in different ways. In this thesis, dynamic models of parallel and series hybrid powertrains are developed, and different strategies for how to control them are compared. An optimization algorithm for decreasing fuel consumption and utilize the battery storage capacity as much as possible is also developed, implemented and tested.

Keywords: Hybrid Electric Vehicle, Modelling, Parallel HEV, Series HEV, Optimization, Prediction

Contents

Abstract	v
1 Introduction	1
1.1 The Hybrid Vehicle Market Today	2
1.2 Purpose of the Thesis	3
1.3 Thesis Outline	3
1.4 Sources	3
1.5 Limitations	3
2 Modelling Hybrid Electric Vehicles	4
2.1 Components Selection	4
2.2 Topologies	5
2.2.1 Parallel HEV	5
2.2.2 Series HEV	7
2.3 Implementation	7
2.3.1 Driver	7
2.3.2 Internal Combustion Engine	8
2.3.3 Electric Machine	9
2.3.4 Battery	10
2.3.5 Generator	11
2.3.6 Driveline	11
2.3.7 Continuously Variable Transmission	13
2.3.8 Vehicle and Environment	13
3 Control strategies	14
3.1 Goal	14
3.2 A Conventional Vehicle	16
3.3 Parallel HEV Control Strategies	16
3.3.1 Excluding Strategy	16
3.3.2 Mixed Strategy	20
3.4 Series HEV Control Strategies	24
3.5 Drive Shaft Oscillations	27
3.5.1 Model	27

3.5.2	Regulation	27
4	Optimization	29
4.1	Considerations and Simplifications	30
4.2	Objective and Constraints	30
4.3	Implementation	34
4.4	Results	34
4.4.1	Zero Prediction Horizon	34
4.4.2	Wider Prediction Horizons	35
4.4.3	Analyzing the Results	36
4.4.4	Validating the Results	44
4.4.5	Usability of the Optimization Algorithm	45
5	Conclusions	46
5.1	Summary	46
5.2	Future Work	46
	References	49
	Notation	51
A	Model parameters	53
B	Simulink models	54

Chapter 1

Introduction

One of the greatest environmental problems of today is air pollution, which is evidenced by the concern over the green house effect and atmospheric ozone layer depletion. Fossil fuel-burning transportation vehicles are some of the largest remaining contributors to air pollution [7]. Purely electric vehicles are seen as a long-term solution to this problem, but existing batteries cannot store enough energy to give a satisfying distance range. Hybrid powertrains were originally conceived as a way to compensate for the shortfall in battery technology, but are today the realistic alternative to combustion engine vehicles. Hybrid electric vehicles are predicted to be an important part of the car industry in the near future. They reduce pollution in the cities, and are more fuel efficient than conventional vehicles.

A hybrid electric vehicle uses two or more power sources, usually a combustion engine and an electric machine. Hereby it combines the range advantage of a conventional vehicle with the environmental benefits of an electric vehicle. The engines can be arranged in different topologies, but the goal is always to reduce fuel consumption and emissions while retaining the performance level.

There are several things that contribute to the environmental advantages of hybrid electric vehicles. First of all, there is the concept of regenerative braking. In a conventional vehicle, the driver controls the speed by either depressing the accelerator pedal to request higher speed, meaning positive torque, or depressing the brake pedal to request lower speed, i.e. negative torque. Positive torque is supplied by the combustion engine, and negative torque by the brakes. In Fig. 1.1, the output power from an engine during a typical 20 minutes driving can be seen. The negative energy constitutes approximately 15% of the total amount of energy that is needed to propel the vehicle dur-

ing these 20 minutes. If this energy had been taken care of, it would have decreased the fuel consumption. In a hybrid electric vehicle, some of this energy is regained. When releasing the gas pedal, the electric motor functions as a generator and uses the kinetic energy to induce a current that recharges the battery and saves the energy for future use. A traditional friction brake is of course also needed, but it can be used to a smaller extent than in a conventional vehicle.

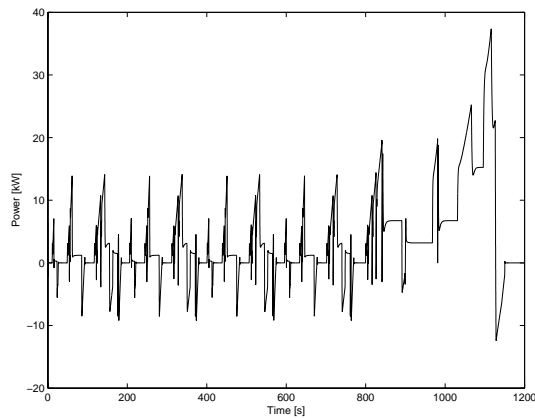


Figure 1.1: Output power from an engine during a typical 20 minutes driving cycle.

The second thing that contributes to the better environmental aspect of hybrid electric vehicles is the so called continuously variable transmission, which is used instead of a conventional step transmission. Where the step transmission would have forced the engine to run at non efficient operating points, the variable transmission softly changes the gear, making it possible to run the internal combustion engine at its most efficient operating point at all times. Finally, the use of two power sources makes it possible to use a combustion engine that is lighter, since it does not have to provide all power by itself.

1.1 The Hybrid Vehicle Market Today

Today there are a few hybrid models on the market, for instance Prius from Toyota and Insight from Honda. Both Prius and Insight have the combustion engine as the primary power source, and the electric motor as assist on startup and acceleration. New models are being developed, and as allowed emission levels decrease, they will become more and more common.

1.2 Purpose of the Thesis

The purpose of this thesis is to develop dynamic models for parallel and series hybrid electric vehicles, and use these models to analyze how different control strategies for power split between the two power sources affect fuel economy. A small investigation on how switching engines causes oscillations in the drive shaft is made, and some proposals for how to obstruct those are given. The use of optimization procedures for decreasing the fuel consumption further is tested and analyzed.

1.3 Thesis Outline

In chapter 2, models for parallel and series hybrid electric vehicles are developed and implemented. The components are described one by one, and the equations that form the basis for the implementation are presented. Chapter 3 deals with different control strategies for when and how to switch engines in the parallel topology, and how to run the engines in the series topology. It is described how the strategies are implemented and what results they bring. In chapter 4, an optimization algorithm for the parallel drivetrain is developed and presented. The results are analyzed and compared to those in chapter 3. Chapter 5 contains some conclusions and proposals for future work.

1.4 Sources

The material used when writing this thesis has been found in the library, on the Internet and many articles have been found in the IEEE database.

1.5 Limitations

Only two topologies are investigated; parallel and series hybrid electric vehicles. The models are unfortunately not tested and validated in a real environment, since there was no access to one. The area of drive shaft torsion and control was very shortly mentioned because of the time limit.

Chapter 2

Modelling Hybrid Electric Vehicles

The vehicle modelling is an important issue that needs to be carefully considered. The difficulty lies in getting a good balance between accuracy and simplicity. The model should be accurate enough for the application, and at the same time not too complicated since that often results in slower simulations. For this application the models must be fast enough to be easily used when developing control strategies. Many articles deal with static models that are built up from maps and static relationships between parameters in the model. These models are comforting since they give fast simulations, but for our intents, a dynamic model that can describe drive shaft oscillations that occur when switching engines is needed. The models are built up from physical equations, and the parameters have been chosen according to existing devices.

2.1 Components Selection

A hybrid electric vehicle, HEV, can be designed in various ways. Common for all designs are that they include two sources of power. These can be for instance combustion engines, electric machines or fuel cells. In this thesis, internal combustion engines and electric machines are going to be used. Research is also made on the possibility to use fuel cells as an alternative to combustion engines, but up to this point a combustion engine is a more realistic alternative. Fuel cells are larger, heavier and more expensive than corresponding combustion engines [1]. All HEV designs also include an energy storage device. Batteries as well as supercapacitors and flywheels are more or less used. Batteries have a limited specific power (measured in kW/kg), regarding absorbing and delivering energy, compared to supercapacitors and flywheels, which

on the other hand have a more limited specific energy (measured in kWh/kg) compared to batteries. In this thesis, only batteries are going to be used as energy storage. The reason is simply that it is the most common energy storage in today's hybrid electric vehicles [1]. Among the different battery types, the nickel metal hydrid battery is a good alternative, since it has a higher specific energy than for instance lead and nickel cadmium batteries.

2.2 Topologies

There are a few recognized types of HEV designs, of which the so called series HEV and parallel HEV are going to be presented and modelled. Another alternative is to combine these two topologies. For instance, the drivetrain can be constructed to partially operate as a series hybrid and partially as a parallel. This would however demand a relatively complex transmission. A third possibility would be to construct a completely mechanical drivetrain by using a flywheel, instead of a battery, as energy storage device. From now on, the focus is going to be on series and parallel hybrids. This is because they are the two most common ones. The two topologies can be viewed in Fig. 2.1 and 2.2.

2.2.1 Parallel HEV

In the parallel hybrid topology, both the internal combustion engine, ICE, and electric machine, EM, are mechanically connected to the wheels. The vehicle can be propelled with the combustion engine, the electric machine, or both of them. Hence, one can choose freely how the engines are going to cooperate to give a sufficient amount of torque at each time. When using only the combustion engine, the electric machine can function as a generator and charge the battery. Since there are few energy conversions, only a small part of the energy is lost and most of it is utilized. Generally, the electric mode is used for city driving. This means that cold starts are avoided in urban areas, which yields acceptable emission levels.

The fixed step transmission is replaced by a continuously variable transmission, CVT. With a CVT, the most efficient ICE operating point for given torque demands can be chosen freely and continuously, in opposite to the fixed step transmission where the gears are discrete. This gives lower fuel consumption levels, since the fuel is used in a more efficient way.

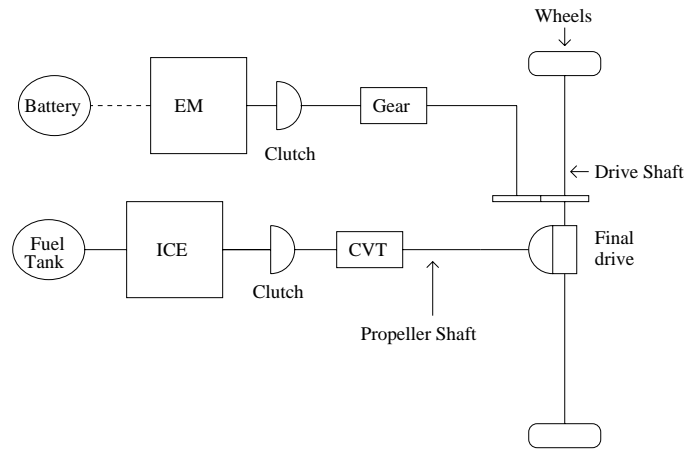


Figure 2.1: Parallel HEV

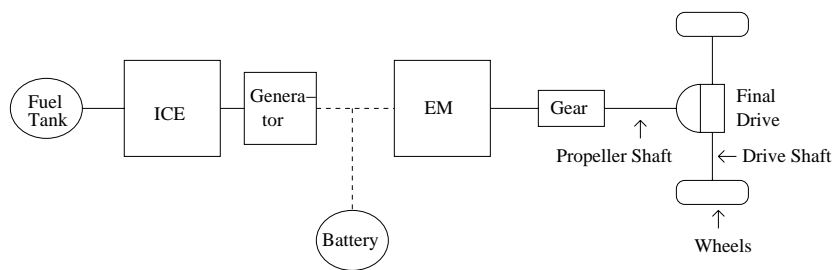


Figure 2.2: Series HEV

2.2.2 Series HEV

A series hybrid electric vehicle uses the internal combustion engine only to charge the battery via a generator. The power needed to drive the vehicle at the demanded speed is taken from the electric machine, while the battery supplies it with the required energy. Hence, no mechanical connection is needed between the ICE and the chassis. If the battery is full, the ICE is turned off, and turned on again when the batteries state of charge is at a minimum level. This technique gives an extra degree of freedom, since the ICE can run at an optimal combination of speed and torque.

One drawback is the two energy conversions that are needed to transport energy from the ICE to the wheels via the generator. Some energy is lost in each conversion because of inner resistances and friction.

2.3 Implementation

The two described HEV topologies are implemented in Matlab/Simulink as in Fig. B.1 and B.2 found in appendix B. The models consist of sub-systems corresponding to the physical components or systems. These are described below. Data and parameters are chosen to make the model as realistic as possible. Therefore most of them origin from the Toyota Prius, a HEV available on the market. A list of parameters can be found in appendix A.

2.3.1 Driver

The driver model is the link between driver and control unit. The speed demand and actual speed are inputs, and the output is a signal that declares how much to accelerate or retard the vehicle. This is simply done with PI-regulators, that decide how much power to take from ICE, EM and brakes respectively.

$$S_{ice} = \max(0, PI(v_{demand}, v_{actual})) \quad (2.1)$$

$$S_{brake} = -\min(0, PI(v_{demand}, v_{actual})) \quad (2.2)$$

$$S_{em} = \alpha v_{demand} + PI(v_{demand}, v_{actual}) \quad (2.3)$$

S_{ice} , S_{em} and S_{brake} are values between 0 and 1, where 1 implies maximum acceleration/brake signal and 0 implies minimum acceleration/brake signal. v_{demand} is the speed demanded by the driver, and v_{actual} is the actual vehicle speed.

2.3.2 Internal Combustion Engine

The internal combustion engine is modelled according to [4]. A short description will be given here. For more details, the reader is referred to [4]. A complete list of variables contained in the model can be found in the notation at the end of this thesis. The model is a so called mean value engine model, i.e. a model where all signals, parameters and variables are averaged over one or several cycles. The inputs are engine speed and acceleration signal from the driver. The outputs are engine torque, air to fuel ratio, from which emissions can be calculated, and fuel consumption. The model accounts for the dynamics of the fuel flow into the cylinders, and also contains a closed loop for injecting the correct amount of fuel corresponding to the demanded air mass flow. It contains a dynamic torque model, where the engine size can be changed by adjusting the displacement volume, and also a dynamic intake manifold model.

The engine model is splitted in several submodels, describing different parts of the engine. The intake manifold model calculates the air flow into the cylinders, \dot{m}_{ac} , with knowledge about engine speed, N , and intake manifold pressure, p_{im} .

$$\dot{m}_{ac} = \frac{\eta_{vol} V_d N p_{im}}{n_r R T_i} \quad (2.4)$$

p_{im} is given from the isothermal model

$$\frac{dp_{im}}{dt} = \frac{R T_i}{V_i} (\dot{m}_{at} - \dot{m}_{ac}) \quad (2.5)$$

where \dot{m}_{at} is the air flow past the throttle, that is proportional to the position of the acceleration pedal. The fuel flow into the cylinders, \dot{m}_{fc} , is the sum of the fuel that goes directly from injection, $(1 - \chi)\dot{m}_{fi}$, and the part that is evaporated from the fuel puddles, $\frac{1}{\tau_{fp}} m_{fp}$.

$$\dot{m}_{fc} = (1 - \chi)\dot{m}_{fi} + \frac{1}{\tau_{fp}} m_{fp} \quad (2.6)$$

The amount of injected fuel is proportional to the air flow into the cylinders, corrected with a factor λ_{reg} to keep the air/fuel equivalence ratio, λ , close to 1.

$$\dot{m}_{fi} = \frac{\dot{m}_{ac}\lambda_{reg}}{AF_s} \quad (2.7)$$

The engine torque production depends on indicated gross work per cycle, W_{ig} , pumping work from the difference in intake and exhaust manifold pressures, W_p , and friction work, W_f .

$$T_{ice} = \frac{W_{ig} - W_p - W_f}{4\pi} \quad (2.8)$$

The pumping work is modelled as

$$W_p = V_d(p_{em} - p_{im}) \quad (2.9)$$

The indicated gross work can be expressed as

$$W_{ig} = m_f q_{HV} \eta_{ig,c} \left(1 - \frac{1}{r_c^{\gamma-1}}\right) \min(1, \lambda) \quad (2.10)$$

The friction work is modelled using the friction mean effective pressure $FMEP$

$$W_f = V_d FMEP \quad (2.11)$$

$FMEP$ is described by

$$FMEP = \xi_{aux} \left(\frac{0.075}{B}\right)^{0.5} [(0.464 + 0.0072 mps^{1.8}) \Pi_{bl} 10^5 + 0.0215 BMEP] \quad (2.12)$$

where $BMEP$ is the brake mean effective pressure. T_{ice} can also be expressed according to

$$T_{ice} = \frac{V_d \cdot BMEP}{2\pi n_r} \quad (2.13)$$

Solving (2.8) to (2.13) above gives an expression for $BMEP$, from which T_{ice} can be calculated.

2.3.3 Electric Machine

The electric machine is modelled as a DC motor with a permanent magnet. The signal from the driver, S_{acc} , the actual engine speed, ω_{em} , and the battery SOC are inputs. The outputs are engine torque, T_{em} , and current, i_{em} . The equations describing the engine according to [5] are

$$T_{em} = i_{em}k_{em} \quad (2.14)$$

$$L_{em} \frac{d}{dt} i_{em} = U_{em} - R_{em} i_{em} - \omega_{em} k_{em} \quad (2.15)$$

$$U_{em} = U_{max} S_{acc} f(SOC) \quad (2.16)$$

where U_{max} is the maximum battery output voltage, and $f(SOC)$ is the influence of the battery's state of charge (SOC) on the battery's output voltage. This nonlinear dependency is modelled as a look-up table according to [9]. The variable k_{em} is the magnetization. R_{em} and L_{em} are inner resistance and inductance respectively.

2.3.4 Battery

The battery model can become quite complex if all of its dynamics is going to be captured. The most important issue when modelling the battery is to capture the decrease in efficiency that arises when the battery loses charge. Therefore, the battery's state of charge and how it affects the battery output voltage needs to be considered. This was done in (2.16). The age dependent efficiency decrease is not taken into account. Within which limits the battery SOC should be varied is a disputed subject. To get a long lifetime, the battery should be allowed to be completely discharged once in a while. Common is however to have a smaller range, since there should always be some energy left for starts, and the battery must not be overcharged because of the risk that it conveys. The equation describing the varying SOC is

$$SOC = SOC_{init} + \frac{1}{Q_{max}} \int_t i(t) dt \quad (2.17)$$

where Q_{max} is the battery maximum charge. This is the most commonly used type in hybrid vehicles. The battery does not need to be charged from the grid. Therefore there is no driving distance limit, except for the size of the fuel tank. The battery in a hybrid vehicle can also be smaller than the one in an electric vehicle. The weight is normally around 1/2 to 1/3 of that of a comparable electric vehicle [7]. The battery has a storage capacity of 6.2 Ah with a maximum output voltage of 273.6 V [2]. Since the maximum discharging current is 80 A and the storage capacity is 6.2 Ah, the battery is discharged in about five minutes at full load.

2.3.5 Generator

In a series hybrid, a generator is needed to transform mechanical energy from the ICE into electrical energy to charge the battery. A loading torque from the ICE makes the generator rotate. A current, that charges the battery, is thereby induced. The equations describing the generator are hence the same as those describing the electric machine, but with the ICE torque as input and a current as output.

2.3.6 Driveline

It is a good idea to study Fig. 2.1 and 2.2 while following the calculations below. The drivetrains look different for the two topologies. In the parallel drivetrain, clutches are required, since both engines are connected directly to the drive shaft. The clutches are used to engage the engines only when needed, so that they do not become an unnecessary load when not used. By considering the subsystems one by one, and using the generalized Newton's second law of motion, equations describing engine and wheel speeds can be found. In the following equations, T denote torques and I inertias. G denote gear ratios. G_{ice} is a variable gear ratio from ICE to final drive. G_{em} is a fixed gear ratio from electric machine to drive shaft. G_f is a fixed gear ratio from propeller shaft to drive shaft. The gearbox and clutch masses are considered to be small in relation to the vehicle mass, so they are neglected. To start with, the flexibility of the shafts is neglected.

Parallel Driveline

Newton's second law of motion for the ICE gives

$$I_{ice}\dot{\omega}_{ice} = T_{ice} - T_{clutch} \quad (2.18)$$

The clutch is assumed to be stiff, and hence it transmits torque and speeds without changing them (except for friction losses, but they are small and therefore neglected). The transmission changes the speed and torque by a factor G_{ice}

$$\dot{\omega}_{propeller} = \frac{1}{G_{ice}}\dot{\omega}_{ice} \quad (2.19)$$

This applies also to the final drive, but with the gear ratio G_f

$$\dot{\omega}_{wheel} = \frac{1}{G_f}\dot{\omega}_{propeller} \quad (2.20)$$

The vehicle and the electric machine are considered to be one subsystem. The wheel speed can be found by solving

$$\begin{aligned} (I_{vehicle} + G_f G_{em} I_{em}) \dot{\omega}_{wheel} &= \\ &= G_f G_{ice} T_{clutch} + G_f G_{em} T_{em} - T_{vehicle} \end{aligned} \quad (2.21)$$

Combining (2.18)-(2.21) gives an expression for T_{clutch}

$$\begin{aligned} T_{clutch} &= \frac{T_{ice}(I_{vehicle} + G_f G_{em} I_{em})}{G_{ice}^2 G_f^2 I_{ice} + G_{em} G_f I_{em} + I_{vehicle}} + \\ &+ \frac{G_{ice} G_f I_{ice} (T_{vehicle} - G_f G_{em} T_{em})}{G_{ice}^2 G_f^2 I_{ice} + G_{em} G_f I_{em} + I_{vehicle}} \end{aligned} \quad (2.22)$$

Using this together with (2.18) and (2.21) results in expressions for wheel speed and ICE speed. The electric machine speed is finally the result of the following equation

$$\dot{\omega}_{em} = G_{em} G_f \dot{\omega}_{wheel} \quad (2.23)$$

The speeds of the ICE, the EM and the wheels are hence the same except for the transmission levels of the connecting devices.

Series Driveline

In the series topology, the driveline equations are easier, since only the electric machine is mechanically connected to the wheels. The electric machine and the vehicle are analysed one by one. The load torque on the machine is denoted T_l . Newton's second law of motion gives the following equations

$$I_{em} \dot{\omega}_{em} = T_{em} - T_l \quad (2.24)$$

$$I_{vehicle} \dot{\omega}_{wheel} = G_f G_{em} T_l - T_{vehicle} \quad (2.25)$$

In the same way as above, the relation

$$\frac{1}{G_{em} G_f} \dot{\omega}_{em} = \dot{\omega}_{wheel} \quad (2.26)$$

is used to find T_l . This results in

$$T_l = \frac{I_{vehicle} T_{em} + G_{em} G_f I_{em} T_{vehicle}}{G_f^2 G_{em}^2 I_{em} + I_{vehicle}} \quad (2.27)$$

Equations (2.24) to (2.27) give expressions for engine speed and wheel speed.

2.3.7 Continuously Variable Transmission

In the parallel topology, a gearbox is needed between ICE and wheels. Instead of a conventional step transmission, a continuously variable transmission is used. As with conventional gear boxes, the gear should be chosen so that the spin rate of the engine is reduced towards the wheels at a rate that makes it possible to move the car at the required speed, and at the same time develop the necessary torque. The CVT works as an automatic gearbox with an infinite number of gears. This makes it possible for the engine to, at all times, choose a gear ratio that lets it work at its optimal operating point. Therefore the vehicle can always run at an environmentally advantageous speed-torque combination. The chosen gear is the ratio between the requested engine speed and the requested wheel speed.

$$G_{ice} = \frac{\omega_{ice,req}}{\omega_{wheel,req}}$$

The required ICE speed is received through an engine efficiency map, and is chosen so that the engine consumes the lowest amount of fuel possible for a given demanded torque.

2.3.8 Vehicle and Environment

The model describes the outer forces acting on the vehicle. A simplified model will be used, where the slope of the road is not considered, and the resistances acting on the vehicle are approximated as a quadratic function of the vehicle speed [4].

$$T_{vehicle} = S_{brake} K_{brake} + a_0 + a_1 v_{vehicle} + a_2 v_{vehicle}^2$$

a_0 , a_1 and a_2 are estimated coefficients and K_{brake} is the brake pedal gain factor. The inertia is described by

$$I_{vehicle} = r_{wheel}^2 m_{vehicle}$$

Chapter 3

Control strategies

3.1 Goal

The main purpose of all of the control strategies is to decrease the fuel consumption compared to a conventional vehicle, without decreasing performance. The main principle is to let the ICE work only when it is at efficient operating points, i.e. good combinations of speed and torque. Since the ICE is fuel efficient when it delivers high torques compared to its maximum torque, and keeps in the middle or lower part of its speed range, the engine should be as small as possible still being able to fulfill the given performance requirements. That means, it should be operating at higher torque areas for larger parts of the driving cycle.

Because of the numerous parameters included in the model it is difficult to give exact results. Changing one model parameter can affect the fuel consumption and other outputs a lot. Therefore, the main focus is the comparison between the different strategies, not the absolute values.

For comparing the performance, two different driving cycles are used. They contain information about demanded speed at different times. The new european driving cycle, NEDC, that can be seen in Fig. 3.1, is a mixture of city driving and country road driving. This is the cycle used for emission certification of light duty vehicles in Europe [3]. Even though NEDC is the most commonly used certification cycle in Europe, it can be interesting to compare the results given from it with the results from other test cycles. A different american test cycle, that contains more low speed sections, is also going to be used, and can be viewed in Fig. 3.2.

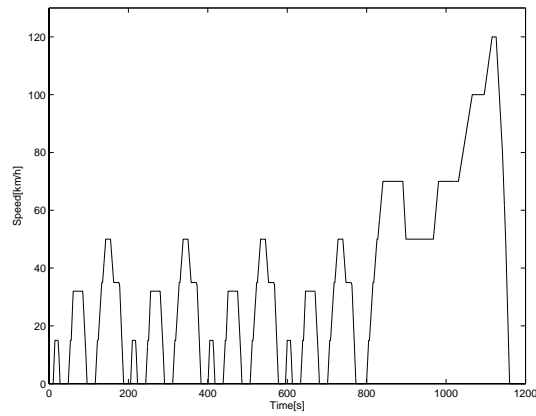


Figure 3.1: The NEDC emission test cycle.

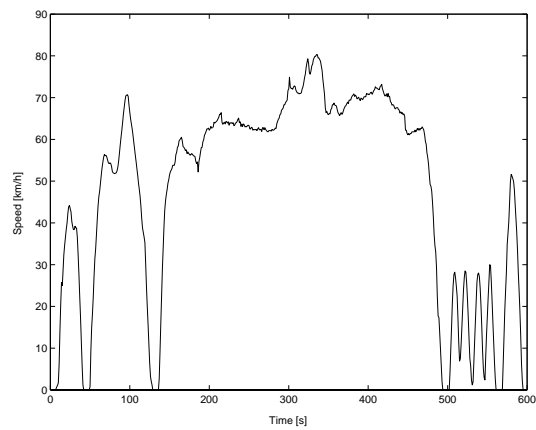


Figure 3.2: The US06 emission test cycle.

3.2 A Conventional Vehicle

To be able to compare results from different control strategies, results from simulations of a classical single-engine vehicle are presented. Interesting parameters are fuel consumption and time spent at different combinations of speed and torque. The fuel consumption for this reference car is 0.84 l per 10 km when using a 2.3 litres engine and running the NEDC. Running the US06 driving cycle instead gives a fuel consumption of 0.75 l per 10 km. As can be seen in Fig. 3.3, where all combinations of torque and speed during one driving cycle (NEDC) has been plotted, the ICE spends much time at operating points where it is inefficient, i.e. low torque areas.

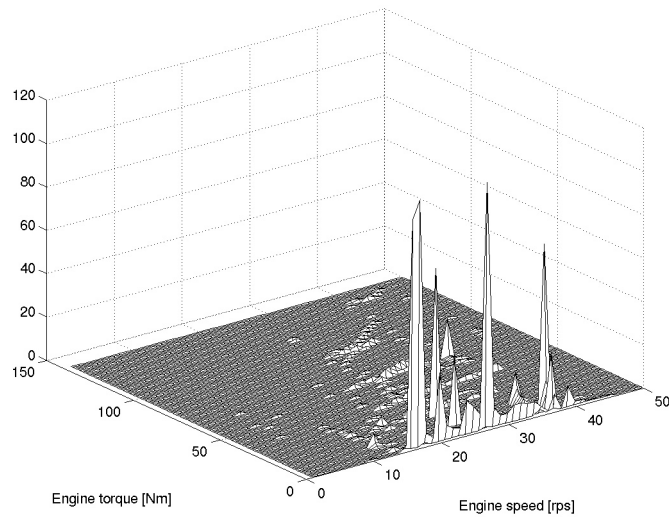


Figure 3.3: Time spent at different operating points by the reference car during NEDC.

3.3 Parallel HEV Control Strategies

With a parallel topology, the power split between the ICE and the EM can be varied in many ways. Important design parameters are the engine sizes and the speed limit that decides when to switch engines.

3.3.1 Excluding Strategy

One possibility is to let the electric machine work alone at low speeds, and only engage the ICE at higher speeds. This strategy bring the

advantage that the ICE can be turned off during stops so that the emission levels decrease. Which speed that should constitute the limit between ICE and EM propelling is a question of importance, and is at first set to 30 km/h, since it is this limit that is most common in today's hybrid electric vehicles. The results from running the european driving cycle can be viewed in Fig. 3.4 to 3.6, where the upper figure displays how the battery SOC changes during the cycle, and the two lower figures display how the power is splitted between the two engines. Naturally, the battery SOC level decreases during periods of EM driving, and increases during periods of ICE driving. Pleasant is that almost all negative power is applied on the EM, which means that the energy is used to charge the battery instead of getting transformed into heat when braking. Less pleasant are the peaks that can be seen in the ICE power diagram. They originate from the switching between the two engines and are a consequence of the sudden torque demand that is put on the ICE, which leads to a too high air flow in to the cylinders in order not to loose speed. The EM is disengaged at 70 km/h, since it is unnecessary to have the battery engaged when it is already full, which is often the case when higher speeds are reached. If using a 1.15 litres engine, the fuel consumption amounts to 0.65 l per 10 km. This means that 0.19 l fuel per 10 km, or 23 %, is saved compared to the reference car.

When running the US06 driving cycle, the engine switching speed limit is raised to 52 km/h. This depends on that there are not as many low speed sections as in NEDC, so if the SOC is going to start and stop at the same level, the speed limit has to be raised. The result of the simulation with this driving cycle can be seen in Fig. 3.7 to 3.9. One can see clearly that the ICE power decreases when the EM power turns zero as the EM is disengaged at speeds higher than 70 km/h. The noisy ICE power diagram depends on the fast speed changes in the high speed zone of the driving cycle. The fuel consumption amounts to 0.69 l per 10 km. One can react on that the battery loses charge quite fast. This is however one of the main advantages when using hybrid vehicles; the battery is much smaller and lighter than that of an electric vehicle and therefore it will be discharged and charged faster.

It was said that the speed limit had to be raised when the US06 driving cycle was used. This is a bit problematic, since the HEV should keep the fuel consumption down for all types of driving. When only using a speed limit as deciding parameter, the electric motor will not be used at all at high speed driving, and very slow driving during long periods will discharge the battery so that the combustion engine has to be used for low speeds. This is a problem that will be addressed in chapter 4.

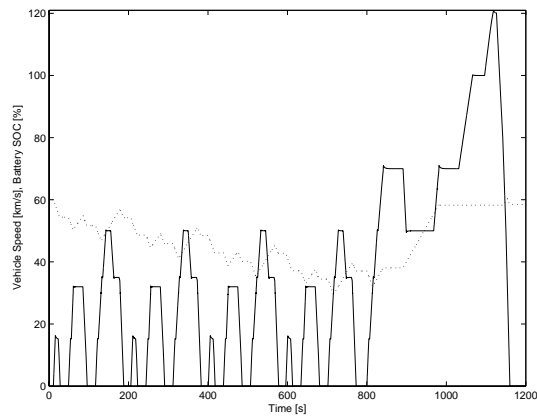


Figure 3.4: Vehicle speed (full line) and battery SOC (dotted line) with NEDC using the excluding parallel strategy.

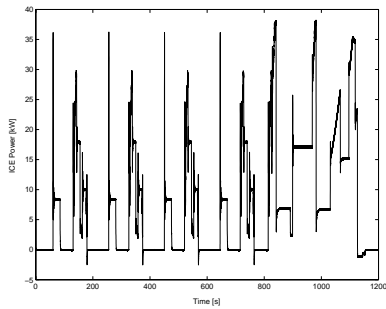


Figure 3.5: ICE power with NEDC using the excluding parallel topology.

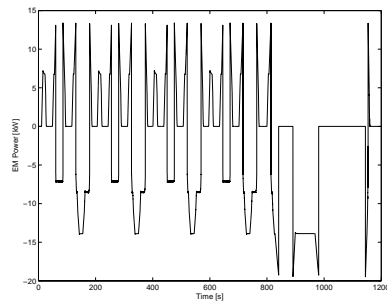


Figure 3.6: EM power with NEDC using the excluding parallel strategy.

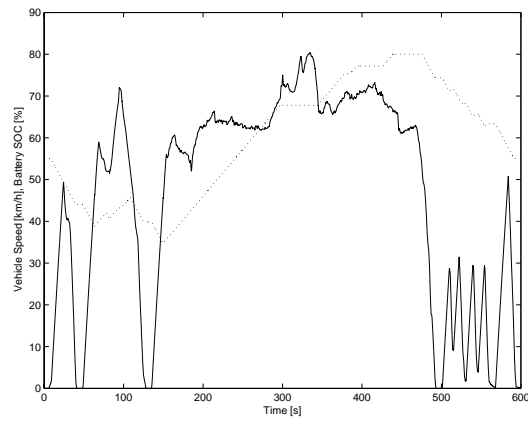


Figure 3.7: Vehicle speed (full line) and battery SOC (dotted line) with the US06 driving cycle, using the excluding parallel strategy.

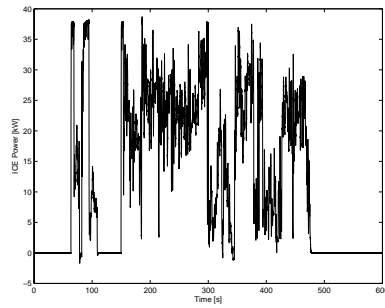


Figure 3.8: ICE power with the US06 driving cycle, using the excluding parallel topology.

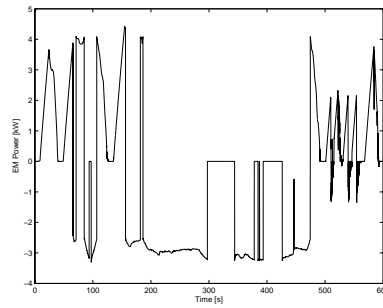


Figure 3.9: EM power with the US06 driving cycle, using the excluding parallel strategy.

It is interesting to see how the CVT works. The gear levels chosen by the CVT are plotted together with the step transmission gears of a conventional vehicle in Fig. 3.10. The CVT follows the behaviour of the step transmission quite well, but changes more softly and often chooses a slightly different gear than the step transmission does.

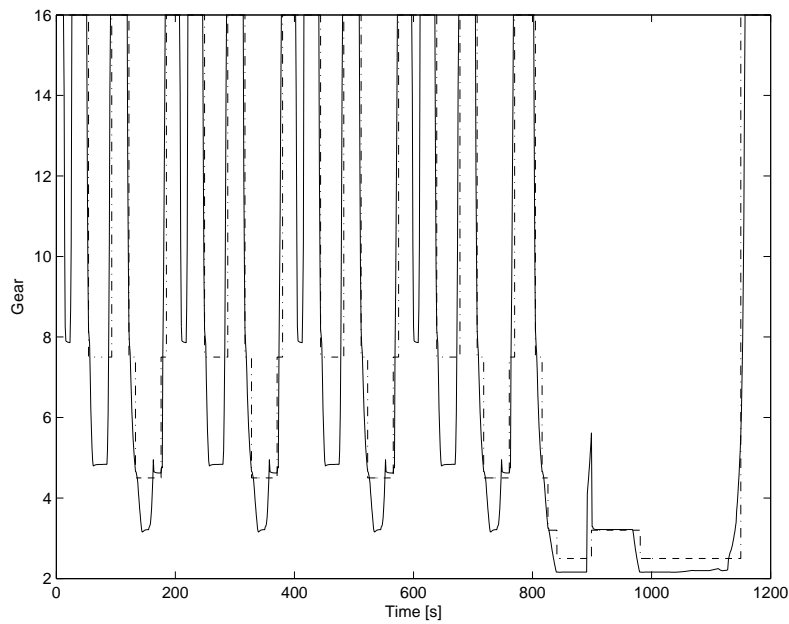


Figure 3.10: Gear levels with a step transmission (dotted line) compared to a CVT (full line) during the NEDC.

3.3.2 Mixed Strategy

The excluding strategy is however not optimal. It was said earlier that the EM should be used as much as possible, but with the excluding strategy it is not used at the end of the NEDC. Therefore another strategy is developed. The excluding strategy is used for low speeds, and the electric machine provides peak power at accelerations and high speeds. This means that the EM is not a load on the ICE at high power areas, but a help. It also offers a possibility to downsize the ICE so that it becomes even more fuel efficient. Here, a 1.15 litres engine is used. The result of this strategy using the NEDC can be seen in Fig. 3.12 to 3.14. The power diagram shows clearly how the ICE power has decreased and the EM power increased at the end of the cycle compared to when using the excluding strategy. The fuel consumption decreases

to 0.56 l per 10 km, i.e. a saving of 33 % compared to the reference car. Using the US06 driving cycle instead, yields the results found in Fig. 3.15 to 3.17. These also show how the decrease in ICE power compared to earlier results. The fuel consumption is 0.55 l per 10 km, that is approximately the same as when running NEDC with the same control strategy.

One question of importance is if the ICE should be turned off or just idle when it is not used. The fuel consumption naturally decreases when the ICE is turned off instead of idling, but if the catalyst loses temperature during this period, it will emit more when started again. This is however a complicated investigation and it will not be discussed further. It is assumed that the ICE is turned off when not used, and that it does not get cold and lose efficiency during shorter periods of non use.

The operating diagram of the ICE is printed in Fig. 3.11. The operating points have clearly moved towards higher torque area, as predicted.

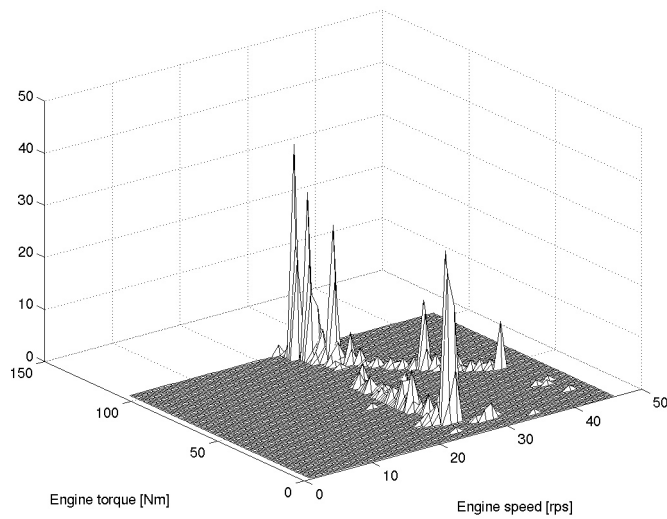


Figure 3.11: Time spent at different operating points with the mixed parallel strategy during NEDC.

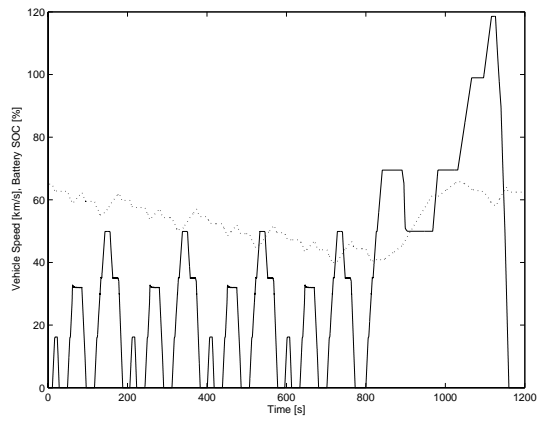


Figure 3.12: Vehicle speed (full line) and battery SOC (dotted line) with NEDC using the mixed parallel strategy.

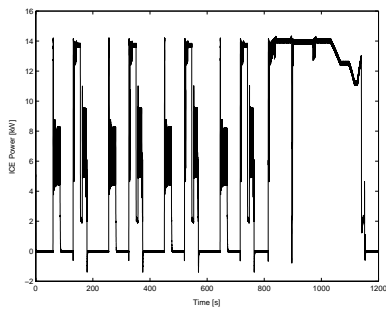


Figure 3.13: ICE power with NEDC using the mixed parallel strategy.

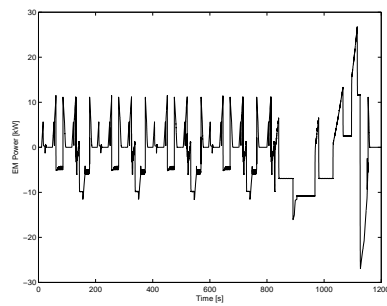


Figure 3.14: EM power with NEDC using the mixed parallel strategy.

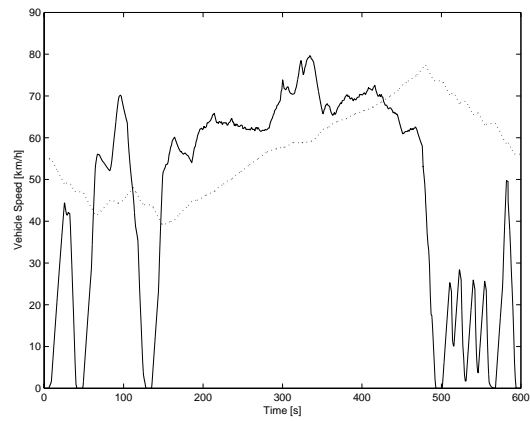


Figure 3.15: Vehicle speed (full line) and battery SOC (dotted line) with US06 using the mixed parallel strategy.

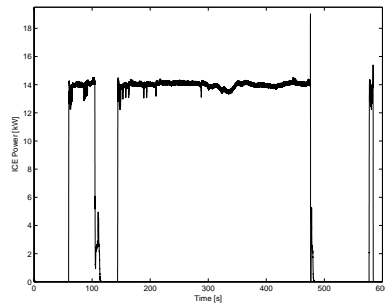


Figure 3.16: ICE power with US06 using the mixed parallel strategy.

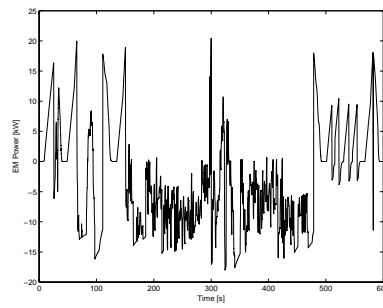


Figure 3.17: EM power with US06 using the mixed parallel strategy.

3.4 Series HEV Control Strategies

Most common in the case of series HEV control strategies, is the so called one point strategy. This means letting the ICE run at an advantageous operating point charging the battery, while the EM is exclusively propelling the vehicle [8]. This makes it possible to use a small ICE, that is lighter and more fuel economic than larger ones. The ICE is turned on when the battery reaches a lower limit, and turned off when the battery reaches a maximum limit. In Fig. 3.18 the vehicle speed and SOC when running the european driving cycle can be viewed. As may be noticed, the battery charging has no connection to the present vehicle speed, except for smaller changes in the charging rate because of changes in power demand from the EM. The battery SOC varies between 40 and 80%. This is a relatively short interval that can be wider. The resulting fuel consumption is 0.50 l per 10 km, using a 1.15 litres engine. The difference in start and end value of SOC is compensated for when calculating the fuel consumption. This is done by running the electric machine until the two values are equal, and adding the distance covered during this time to the total distance covered during the driving cycle.

Problematic in the case of series hybrid electric vehicles, is the fact that the battery can be discharged faster than it can be charged. Therefore, at times when the battery is charged by the combustion engine, the electric motor must not consume more current than is flowing into the battery during longer periods, since that could deplete the battery. This can be seen in for example Fig. 3.18. If the car is accelerating during periods of battery charging, the current flowing into the battery is lower than the one flowing out of it, which makes the battery SOC curve fall slightly before it continues going up. In Fig. 3.19 and 3.20, the power delivered by the ICE and the EM can be viewed.

With the US06 driving cycle, the results in Fig. 3.21 to 3.23 are achieved. The fuel consumption amounts to 0.49 l per 10 km, when the difference in SOC between start and end of the cycle has been compensated for.

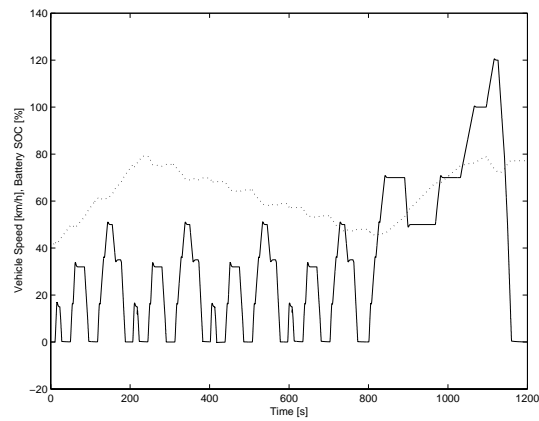


Figure 3.18: Vehicle speed (full line) and battery SOC (dotted line) for the series topology, using the NEDC.

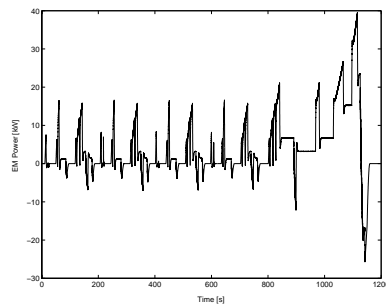


Figure 3.19: EM power for the series topology, using the NEDC.

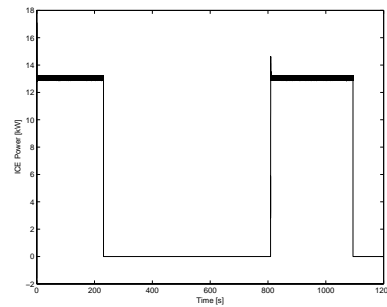


Figure 3.20: ICE power for the series topology, using the NEDC.

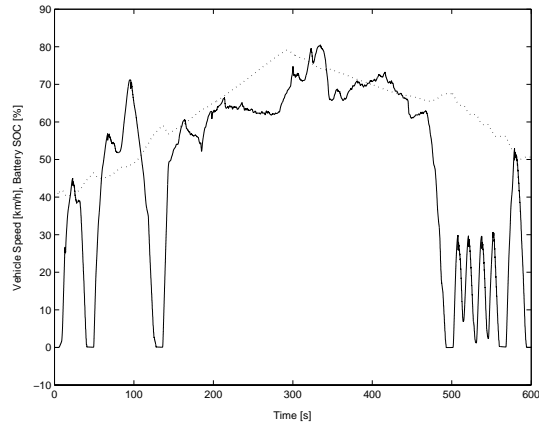


Figure 3.21: Vehicle speed (full line) and battery SOC (dotted line) for the series topology, using the US06 driving cycle.

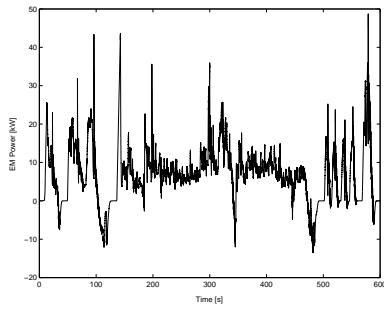


Figure 3.22: EM power for the series topology, using the US06 driving cycle.

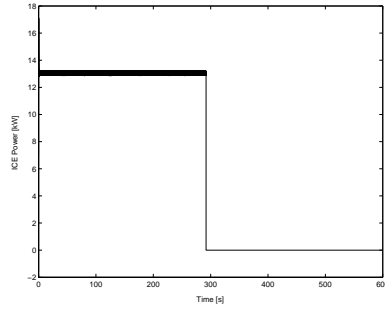


Figure 3.23: ICE power for the series topology, using the US06 driving cycle.

3.5 Drive Shaft Oscillations

So far, a stiff drive shaft has been assumed. The simplification that this assumption brings has made the modelling and regulator development easier than it would have been otherwise. In reality, the shafts are not stiff. When a torque is applied at one end of the shaft, an angle difference between the ends will appear. A larger torque gives a larger angle difference. In single-engine vehicles, this drive shaft flexibility causes a problem when shifting gear, a problem that is addressed in for instance [6]. The problem is that the difference in engine torque that rises when shifting gear makes the shaft start oscillating.

One can expect that the same problem will arise when shifting between the two engines in a parallel hybrid electric vehicle. Disconnecting one engine and connecting the other gives a torque change that will probably cause oscillations. To see how they behave, the old drive shaft model is replaced with a new dynamic one. It should be mentioned that other components, such as clutch, gearbox and propeller shaft, also are flexible. The critical point in our system is however the drive shaft since it is there the engines are connected.

3.5.1 Model

The drive shaft is modelled as a damped torsional flexibility, having stiffness k and internal damping c [6]. Those parameters are dependent on what material the shaft is made of. Clutch, transmission and propeller shaft are all assumed to be stiff.

$$T_{wheel} = T_{drive} = k(\theta_{final} - \theta_{wheel}) + c(\dot{\theta}_{final} - \dot{\theta}_{wheel}) \quad (3.1)$$

θ_{final} is the speed of the shaft at the point where the engines are connected to the shaft. Implementing this equation in the existing model gives rise to the oscillations that can be viewed in Fig. 3.24. The damping and amplitude of the curve is strongly dependent on the material of the shaft, but the general behaviour is that of the curve in Fig. 3.24.

3.5.2 Regulation

The oscillations following from switching between the two engines are unwanted for two reasons. First of all, oscillations with too high amplitude can result in damages on the shaft. Secondly, the sudden changes and oscillations in speed, eventhough small, can be unpleasant for the driver. Normally, a regulator exists that calculates how much fuel to inject to reach the demanded speed at the present state. This regulator is however dependent on the driver and cannot be used for this

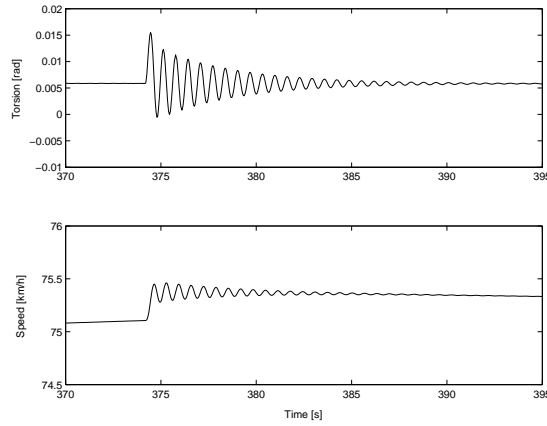


Figure 3.24: Drive shaft and vehicle speed oscillations that occur when shifting engine.

purpose. Therefore, a regulator can be developed, that adds an input to the accelerator signal given by the driver, that compensates for the oscillations by making the engine inertia work in the opposite direction of the oscillations, at the same time as the desired speed is obtained. This can be done by implementing a PID-regulator on the following form

$$U = P_{acc} + PID(\dot{\theta}_{final} - \dot{\theta}_{wheel}) \quad (3.2)$$

It calculates a correction term (to be added at both engines input signals) from knowledge about the present difference in drive shaft angular speed. To make the switch as smooth as possible, the control signals can overlap each other. This means that the engine connected to the drive shaft is not disconnected at the same moment that the other engine is connected, but a bit later. This gives a slower, more convenient and for the shaft less harmful switch between the two engines. A better control strategy would be to use zero-torque switch. This means that the drive shaft torque is regulated to zero before the engine switch, so that the shaft transmits zero torque during the switch, raising the torque again afterwards. This would give a smoother shift, since there would not be a sudden change in torque.

Chapter 4

Optimization

If a vehicle is equipped with a navigation device, for instance a GPS, it can receive information about the driving environment ahead of it. Modern digital road maps contain information about road topography and speed limits, and sensors can detect distance to obstacles around the car. If the driver can load information about his planned route into a control unit, connected to a navigation device, a prediction of the power needed to drive the car for a specific time can be made. Information about the predicted power demand can be used to compute the optimal way of splitting the power between the two energy sources, in order to minimize fuel consumption and emissions. The obvious solution to this problem would be to apply as much electric torque as possible, but that would eventually deplete the battery. Other approaches, such as the ones discussed in chapter 3, are better, but do not necessarily result in a balance of net charge in the battery. With access to information about future and past power demands, the power split can be made in a more controlled way. For instance, if there is a steep hill in front of the car, it is a good idea to charge the battery in advance so that it can provide extra power when going uphill.

In a simulation environment this theory functions perfectly, but in reality it is likely that the route will be disturbed by unexpected events. However, using information about the route ahead with a bit of caution, is helpful when trying to find the most fuel economic way of driving. One can easily predict, that the fuel consumption will decrease when longer predictions are made. But how it decreases and how the control unit chooses to split the power is not that obvious. Investigating how the use of predictive optimization techniques affects fuel economy is the purpose of this chapter. The parallel hybrid is the most complicated and challenging topology to control, and is therefore the focus of our study.

4.1 Considerations and Simplifications

The task of splitting the power demand between the two energy sources can be formulated as an optimization algorithm. For this purpose, a simpler HEV model is stated. Since the model will be included in the algorithm, it cannot be too complex. The algorithm has to be fast enough to be performed in real-time during driving.

The problem is posed as a nonlinear convex optimization problem. The convexity guarantees that the found minimum is global. The problem is non-causal in that it finds the minimum fuel consumption using knowledge about future and past power demands. One of the most important issues arising is to keep the number of variables and constraints down. The 1200 seconds long NEDC driving cycle is used, and the sample time is set to 1 second. The maximum prediction length is hence 1200 seconds, and therefore the input vectors to the optimization algorithm have a maximum length of 1200 elements. This means that every new variable used will give maximum 1200 extra variables in the algorithm and every new constraint will give maximum 1200 extra constraints on the variables. Hence, it is easy to understand that keeping the problem small is important for the usability of the program. Some simplifications are made in order to reduce the complexity of the system and maintain a description that is convex.

- The fuel consumption is a convex function of the ICE power and efficiency.
- The ICE power only takes positive values. Negative ICE power is instead applied on the brakes. The fuel consumption at non-positive ICE power is hence the same as when idling.
- The voltage on the EM is assumed to be constant 273.6 V. This means that the EM is either fully used or not used at all, no states inbetween are possible.
- The electric motor efficiency is constant.
- The battery's storage efficiency is constant. It does not change with the state of charge or power levels.

4.2 Objective and Constraints

The HEV model is implemented as constraints in the optimization problem. The first constraint is the balance between needed and given power. The power taken from the ICE and EM, $P_{ice}(t)$ and $P_{em}(t)$,

must at all times sum up to the power needed to propel the vehicle, $P_{prop}(t)$.

$$P_{prop}(t) = P_{ice}(t) + P_{em}(t) + P_{brake}(t) \quad (4.1)$$

P_{prop} was taken from the QSS toolbox, a model library containing quasi-static models of several vehicle topologies. There, P_{prop} is calculated from

$$P_{prop} = F_w v = v(m\dot{v} + F_a + F_r) \quad (4.2)$$

where F_a and F_r are air and roll resistances, and v is the vehicle speed. This means that the vehicle model used only has one state. $P_{brake}(t)$ is the power that is lost when the brake pedal is used to slow down the vehicle. Naturally, $P_{brake}(t)$ only takes negative values. The brake pedal should of course be used as seldom as possible, but sometimes it is inevitable. One example is when the battery is already full and the vehicle has to be retarded. Another is if using only the engine as brake is not effective enough, but the car has to be retarded faster.

A second consideration is how the power taken from the EM affects the battery's state of charge.

$$P_{em}(t) = -\eta_{em} Q_{max} U_{em} \frac{d}{dt}(SOC(t)) \quad (4.3)$$

Q_{max} is the maximal battery charge and U_{em} is the voltage taken from the electric motor. Observe that since U_{em} is constant, limitations on $P_{em}(t)$ also puts limitations on the rate at which the battery is charged and discharged.

Further, the sum of the charging and discharging of the battery must be zero. This is achieved by constraining the battery SOC to be equal in the first and last sample of the prediction interval. This makes it possible to compare the fuel consumption to that of a conventional car.

$$SOC(t_{stop}) = SOC(t_{start}) \quad (4.4)$$

The objective of the optimization is the minimization of the total fuel consumption, Ψ .

$$\Psi = \int \psi(t) dt \quad (4.5)$$

The fuel consumption in each time step, $\psi(t)$, can be calculated from the equation below, where η_{ice} is the ICE efficiency and q_{HV} is a thermodynamical constant expressing the energy density in a specific fuel (measured in J/kg).

$$\psi(t) = \frac{P_{ice}(t)}{\eta_{ice}(T_{ice}(t), \omega_{ice}(t))q_{HV}} \quad (4.6)$$

A problem that arises is how to implement η_{ice} 's dependency on torque and speed. The equation

$$P_{ice}(t) = T_{ice}(t) * \omega_{ice}(t)$$

has to be avoided in the algorithm, since it is not a convex function. However, the problem disappears if a relationship between speed and torque can be found, so that η_{ice} can be expressed as a function of P_{ice} alone. The efficiency map of an engine of appropriate size can be seen in Fig. 4.1. This efficiency map was found in the QSS toolbox. In Fig.

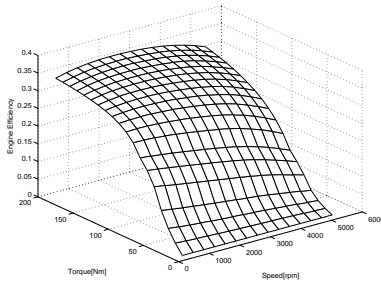


Figure 4.1: Engine efficiency for different combinations of speed and torque. The engine is most efficient for high torques.

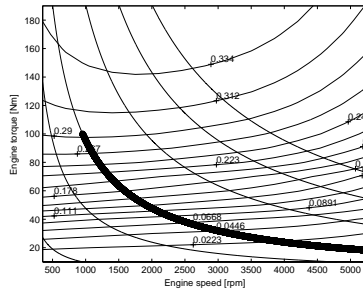


Figure 4.2: Fig. 4.1 drawn from above. The horizontal slightly curved lines illustrate fuel efficiency levels. The diagonal lines are lines on which the power is constant.

4.2, the same efficiency map is drawn from above. The section of the constant power curve (corresponding to 10 kW) that is marked with a bold line, represents the torque-speed combinations that can be reached within the gear limits at the present vehicle speed. In this example it is assumed that the vehicle is driving at 5 km/h, requiring a torque of 200 Nm, which could for instance be the case when just starting from a still position. One can see that in this example the highest efficiency cannot be reached. Even if the best possible speed-torque combination is chosen, the efficiency is below 0.3. Generally, when driving at

low speeds higher and more efficient gears are impossible to engage, since that would make the engine stop. Hence, how close to the highest efficiency curves we can come depends on the present wheel speed. Typically, high efficiency can not be reached at low speeds.

To sum up, η_{ice} can be approximated as a polynomial of P_{ice} , if also considering whether the wanted combination of speed and torque can be reached. An approximation is made by stating that the engine is inefficient at lower power (low speeds). η_{ice} is hence stated as a nonlinear function of P_{ice} alone. Equation (4.6) can then be rewritten so that ψ is expressed as a function of P_{ice} . This function is slightly nonlinear, but can be approximated by a linear function according to (4.7). In this equation, the fuel consumption is measured in litres per second.

$$\psi(t) = 10^{-3}(0.1026 + 0.0001P_{ice}) \quad (4.7)$$

The constants are estimated in Matlab. The fuel consumption during the whole route can then be determined by integrating equation 4.7.

$$\Psi = \int_{t_{start}}^{t_{stop}} 10^{-3}(0.1026 + 0.0001P_{ice})dt \quad (4.8)$$

Equation (4.8) constitutes the objective function of the optimization algorithm. Observe that the CVT simplifies the construction of the optimization algorithm. The procedure described above would not have been possible if a CVT was not included. Without a CVT, the fuel consumption would also depend on which gear that was engaged at different speeds.

Other constraints are imposed on the problem variables because of physical limits and design matters. These are limits on power produced by both engines, brake power and battery state of charge.

$$\begin{aligned} P_{ice}(t) &\leq P_{ice,max} \\ P_{ice}(t) &\geq P_{ice,min} \\ P_{em}(t) &\leq P_{em,max} \\ P_{em}(t) &\geq P_{em,min} \\ P_{brake}(t) &\leq P_{brake,max} \\ P_{brake}(t) &\geq P_{brake,min} \\ SOC(t) &\leq SOC_{max} \\ SOC(t) &\geq SOC_{min} \end{aligned}$$

4.3 Implementation

The optimization is carried out with help from Matlab's Optimization Toolbox. The optimization is done with a command called *fmincon*. The command accepts both linear and nonlinear objective and constraints. To make the process faster, the gradients of the equations are precalculated by hand and are sent together with the equations and a starting solution to the optimization algorithm. The problem has been discretized, which means that approximations of derivatives and integrals have to be made. Derivatives are approximated by

$$\frac{d}{dt}x(t) \approx \frac{x(k(T_s + 1)) - x(kT_s)}{T_s} \quad (4.9)$$

Integrals are approximated by

$$\int_{t_{start}}^{t_{stop}} x(t)dt \approx T_s \sum_{k_{start}}^{k_{stop}} x(kT_s) \quad (4.10)$$

T_s is the sample time, which will normally be 1 second in our calculations. The complete optimization algorithm is stated in table 4.1.

4.4 Results

The time span that we assume knowledge about is called the prediction horizon. The prediction horizon is varied between 0 and 1200 seconds. As mentioned, the total power needed to propell the vehicle is given from the QSS toolbox. The needed power is computed from an assumed vehicle mass of 1700 kg.

4.4.1 Zero Prediction Horizon

First of all, the prediction horizon is set to zero. This means that there is no possibility to vary the state of charge and hence no possibility to run the electric machine. This is done to see what the fuel consumption of a reference car is, so that the results achieved with wider prediction horizons can be compared to this. The maximum ICE power is set so that the ICE alone can propell the vehicle over the whole route. It should be mentioned that the engine map used to compute the fuel consumption is created with data from a fuel map of a smaller engine, scaled to get the right proportions. This might result in slightly uncertain values for those simulations where the ICE power takes high values. But as we will see, this only happens when using zero seconds prediction horizon. With zero seconds prediction horizon the fuel consumption amounts to 0.593 l per 10 km. The power split and the battery SOC can be viewed in Fig. 4.4.

Objective:

$$\text{minimize}(T_s \sum_{k=k_s}^{k_f} \psi[kT_s])$$

Constraints:

$$\begin{aligned} \psi[kT_s] &= 10^{-3}(0.1026 + 0.0001 * P_{ice}[kT_s]) \\ P_{prop}[kT_s] &= P_{ice}[kT_s] + P_{em}[kT_s] + P_{brake}[kT_s] \\ \frac{1}{T_s}(SOC[k(T_s + 1)] - SOC[kT_s]) &= -\frac{1}{Q_{max}U_{em}\eta_{em}}P_{em}[kT_s] \\ SOC[k_{final}T_s] &= SOC[k_{start}T_s] \\ P_{ice}[kT_s] &\leq P_{ice,max} \\ P_{ice}[kT_s] &\geq P_{ice,min} \\ P_{em}[kT_s] &\leq P_{em,max} \\ P_{em}[kT_s] &\geq P_{em,min} \\ P_{brake}[kT_s] &\leq P_{brake,max} \\ P_{brake}[kT_s] &\geq P_{brake,min} \\ SOC[kT_s] &\leq SOC_{max} \\ SOC[kT_s] &\geq SOC_{min} \end{aligned}$$

Table 4.1: Complete optimization algorithm.

4.4.2 Wider Prediction Horizons

With short prediction horizons, the optimization algorithm is quick and usable. Optimization with longer prediction horizons can hardly be realized with the present implementation of the algorithm. Therefore, it is worth to investigate the rate at which the fuel consumption decreases for wider prediction horizons. In the table below, a comparison is summarized. The different horizon lengths compared are 10, 30, 60, 80, 100, 120, 300 and 1200 seconds respectively. The reason for choosing those lengths is that they best capture the resulting improvement in fuel economy. In all cases, the demand that the battery SOC has to start and end at the same level (60%) in each optimization interval is fulfilled. Hence, the results are comparable. In table 4.2, the achieved results are summarized. Observe that these results are compared to a car having a smaller engine than the reference car used in chapter 3.

Comparing them to the reference car gives even better percentual improvement. For the largest horizon, the sample time has been increased, since the algorithm was too large and slow otherwise. The difference that this simplification conveys has been tested by running the algorithm with increased sample time for shorter prediction horizons, and is taken into consideration by multiplying the fuel consumption with this correction factor.

PH[s]	FC[l/10km]	I[%]
0	0.593	0.0
10	0.582	1.9
30	0.551	7.1
60	0.512	13.7
80	0.478	19.4
100	0.471	20.6
120	0.469	20.9
300	0.468	21.1
1200	0.465	21.6

Table 4.2: Optimal fuel consumption for different prediction horizons. The first column contains the used prediction horizon, the second holds the minimized fuel consumption, and the last column displays the relative improvement, expressed as a percentage, compared to having zero prediction horizon.

In Fig. 4.3, the improvement in fuel consumption is plotted against corresponding prediction horizon. The figure clarifies that the largest improvement is gained when approaching 100 seconds horizon. Above 100 seconds the profit is small. The power split between the two engines and the brake pedal together with the battery use can be viewed in Fig. 4.5 to 4.8 for some of the investigated prediction horizons.

4.4.3 Analyzing the Results

As predicted, the fuel consumption decreases with increasing prediction horizon. Interesting is that the first few minutes of knowledge about the driving route ahead seems to make the largest contribution to better fuel economy. This is pleasant, since it is more probable that we have correct information about the nearest driving environment, and thereby a better opportunity to do a more correct prediction. The fact that the optimization is done only on NEDC is of course contributing to the results, since this cycle consists of four rather similar blocks. With

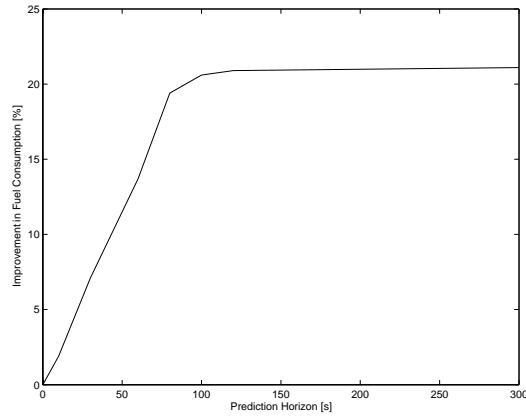


Figure 4.3: Improvement in fuel consumption.

120 seconds prediction horizon, the EM is almost utilized as much as possible. When widening the horizon further, the fuel consumption is not decreased much more. Making predictions longer than a few minutes is hence with the existing software not worth the trouble, since it brings a slower algorithm but hardly any improvement in fuel consumption.

In Fig. 4.8 it can be seen, that the optimal result seems to include a rather flat and low distribution of ICE power over the route. This is natural, since the optimal solution should include that the ICE lies constant at the average power required, if no constraints on the EM or battery are active. An interesting expansion of the developed algorithm, that might change this result, would be to also include minimization of the emissions in the objective.

There seem to be several solutions to the optimization problem that are approximately equally good. With larger prediction horizons, the fuel consumption is not changed much, even if it is clear that the solutions are different. This might depend on that the objective function surface is quite flat around the optimal point.

The sizes of electric machine and battery are the most limiting factors for the decrease of the fuel consumption, especially when using large prediction horizons. Since there is a limitation on both positive and negative current, i.e. discharging and charging rate of the battery, there is a limit on the result. The reason for having to apply a negative power on the brake at the end of the driving cycle is the limitation on the current allowed to flow into the battery. In Fig. 4.4 it can be

seen that the actual negative power that is needed to slow down the car from 120 km/h to 0 km/h is approximately -40 kW. With 1200 seconds horizon, this negative power is split between generator and brakes in an optimal way, since the generator can only receive 50 A charging current, which corresponds to -17 kW power. This is also the power received by the generator. The rest is applied on the brakes. Larger electric machines and batteries can endure larger negative currents. In the driving cycle used, it had been possible to take care of the energy lost at the end of the cycle if having larger battery and electric machine. A test shows that by allowing 1.5 times higher current flowing into and out from the battery, the fuel consumption is decreased by 23.8% instead of 20.6% for 100 seconds prediction horizon.

One should also mention that the optimal power split according to this model, gives a result that looks more like the results of a series hybrid than the result of a parallel hybrid. In fact, the power split achieved with the optimization algorithm looks much like the result of a series hybrid but with a smaller electric machine that needs some help at heavy load.

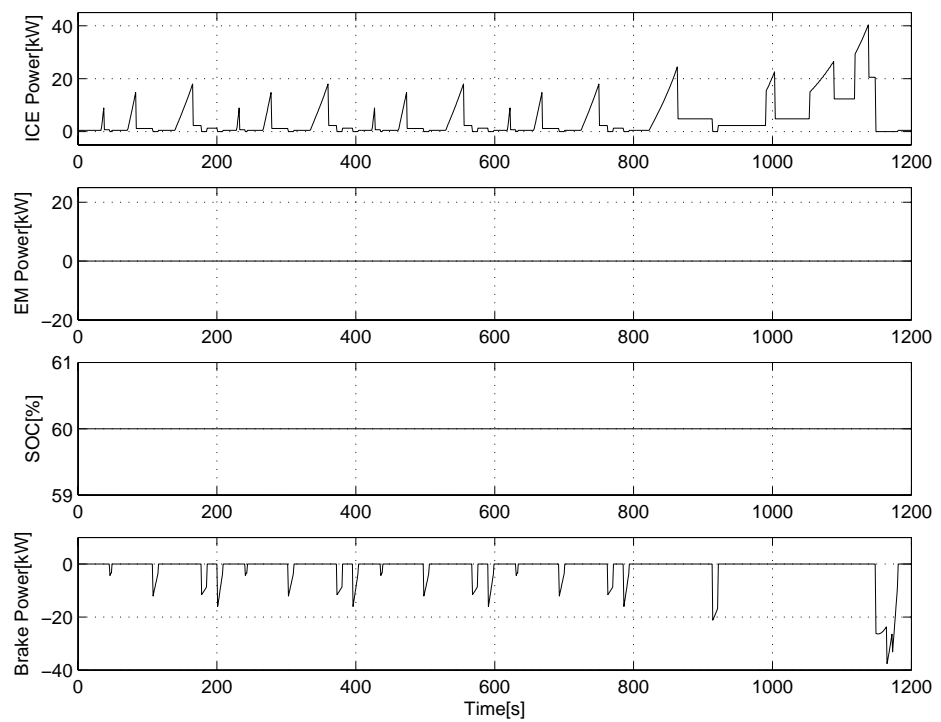


Figure 4.4: Power split and battery use when using no prediction horizon. All positive power is applied by the ICE and all negative power is absorbed by the brakes.

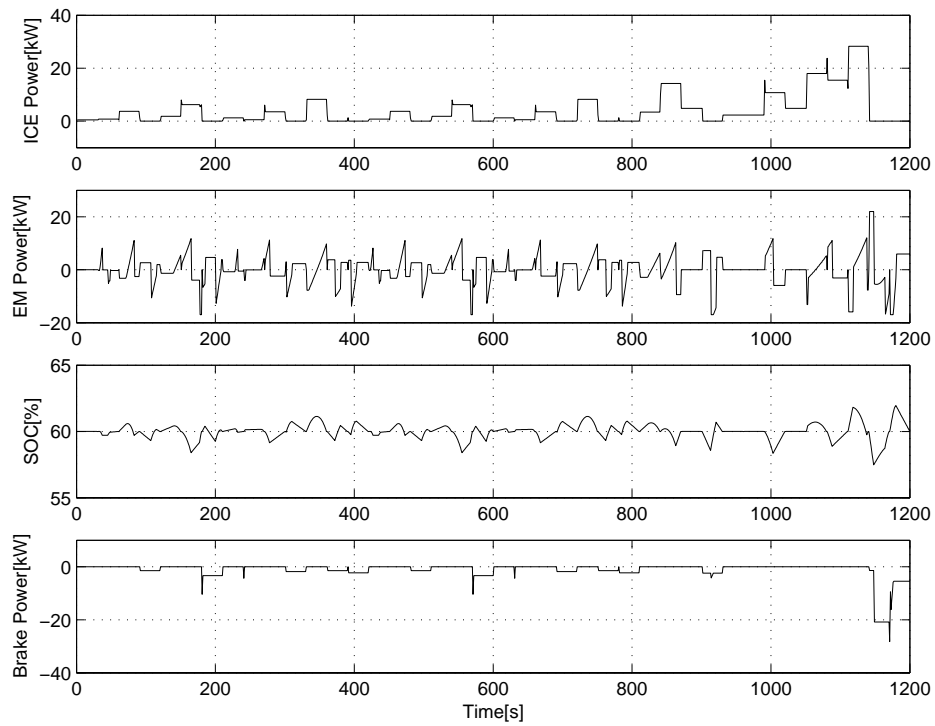


Figure 4.5: Power split and battery use in the case of 30 seconds prediction horizon. Some of the power is applied on the EM instead of ICE and the brakes. The prediction horizon is yet however too short for the system to fully utilize EM and battery. As one can see, the battery SOC interval is very small.

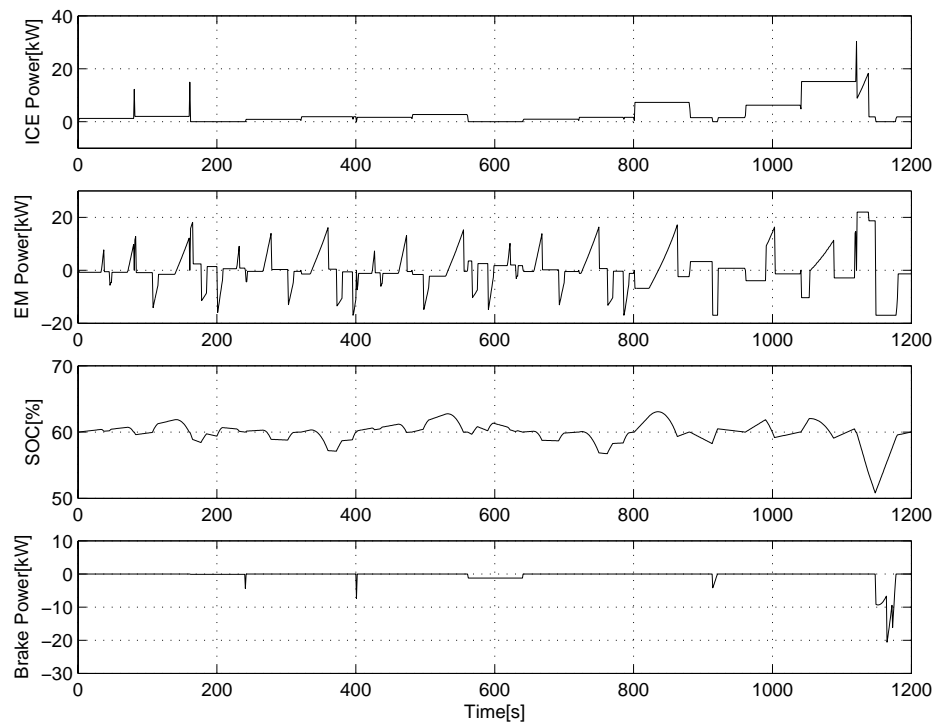


Figure 4.6: Power split and battery use in the case of 80 seconds prediction horizon. The usability of battery and EM is starting to become visible. The SOC interval is increasing and the brake pedal is not used much.

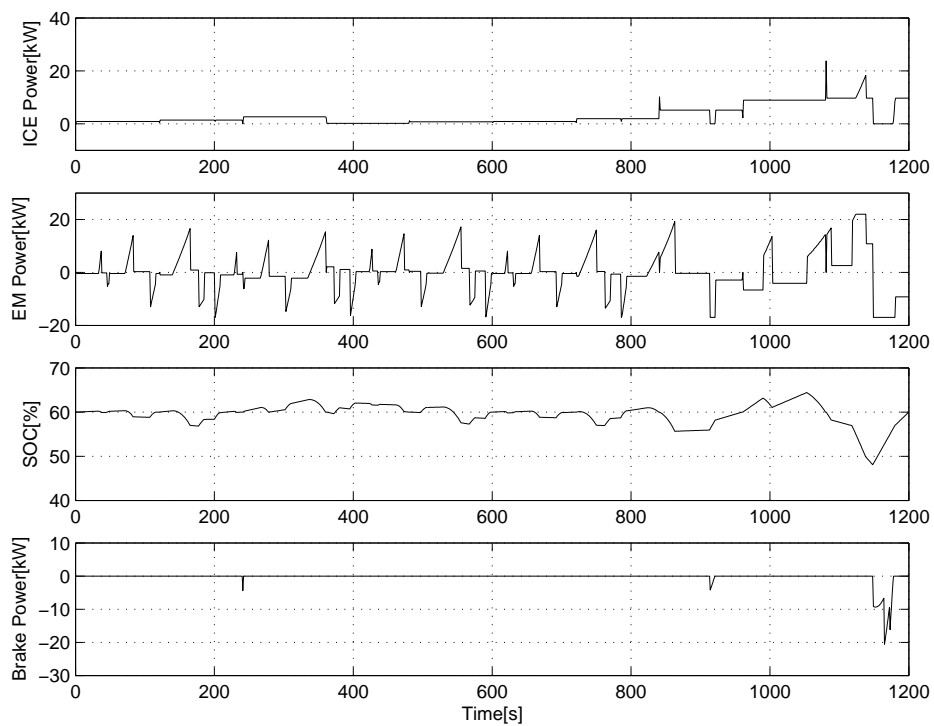


Figure 4.7: Power split and battery use in the case of 120 seconds prediction horizon. The EM is almost fully utilized.

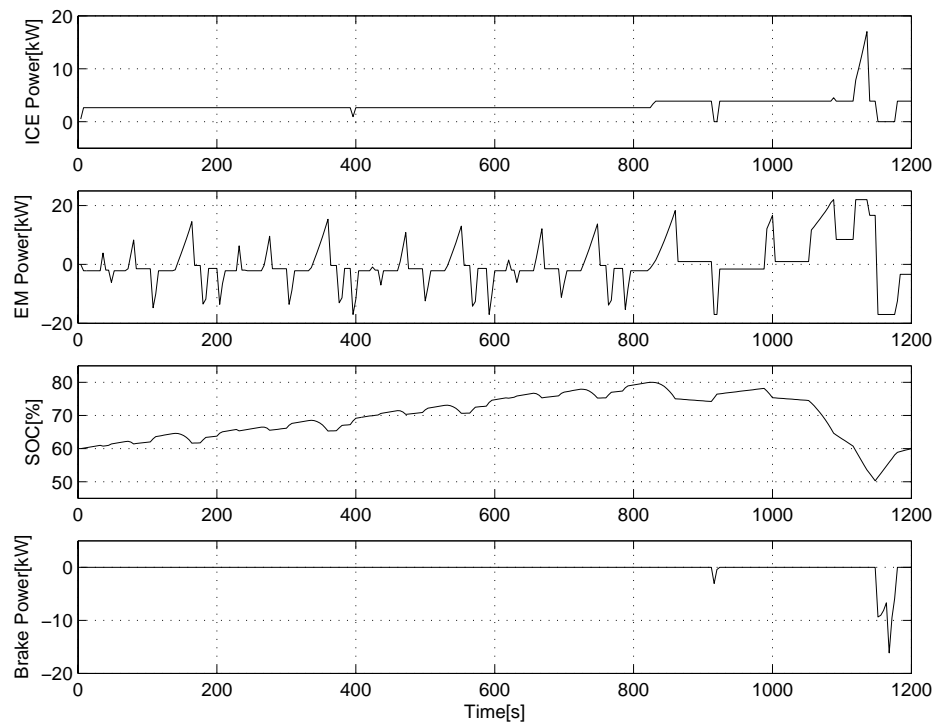


Figure 4.8: Power split and battery use in the case of 1200 seconds prediction horizon. The widest horizon does not contribute to a much better fuel economy than the former, even though the battery SOC interval is wider.

4.4.4 Validating the Results

Finally, the optimal power split achieved from the static optimization model is applied to the dynamic model developed in chapter 2. This is done to see if the result from the optimization is valid also in a more realistic environment. The application of the power split is done by controlling the combustion engine so that it delivers approximately the precalculated combustion engine power, and controlling the electric machine so that the given driving cycle is followed. The engine size is set to 1.15 l. With those inputs the fuel consumption is decreased to 0.44 l per 10 km, which is approximately the same as the predicted result of the optimization algorithm. In Fig. 4.9, it can be seen how the battery state of charge curve, when applying the precalculated power split on the dynamic model, fits the precalculated battery state of charge curve. This figure should of course be compared to the SOC curve in Fig. 4.8. The behaviour of the curves are the same, but they do not follow eachother exactly. The differences probably depends on the much simplified model used in the optimization algorithm, that cannot capture all of the dynamics that the dynamic model can. However, it is satisfactory that the fuel consumption decreased to approximately the same level as was precalculated.

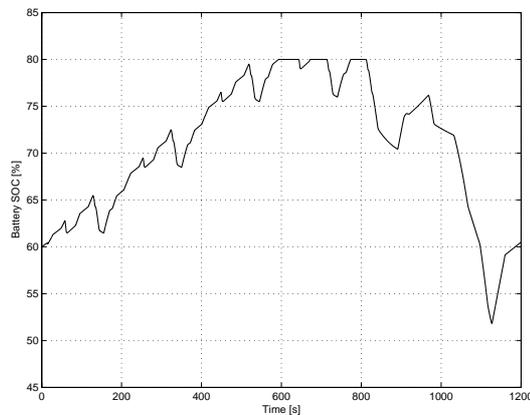


Figure 4.9: The battery state of charge over time when the optimal power split is applied on the dynamic model.

4.4.5 Usability of the Optimization Algorithm

The optimization algorithm is intended to be used in a so called model predictive control (MPC) strategy. This means optimizing online in each time step, using a prediction horizon long enough to yield good results. The first element of the resulting power split vector should then be applied as inputs to the control unit, that consequently gives signals to the both power sources telling how much power to produce. For this purpose, the implemented optimization procedure has to be much faster, since it should be performed on-line during driving.

Chapter 5

Conclusions

5.1 Summary

The control strategies developed in chapter 3 gave good results regarding the decrease in fuel consumption. For the parallel powertrain, the control laws brought an insecurity in that the battery state of charge level showed to be sensitive to the speed limit that decides when to propel the vehicle with combustion engine and electric machine respectively. A too high limit depleted the battery, while a too low limit made the combustion engine run even though the battery was fully charged. This problem was addressed in chapter 4, where an optimization algorithm was developed that kept track of the battery state of charge and gave good results regarding the fuel consumption. Interesting was also that there seemed to exist a time limit, where longer prediction horizons did not give any better results. This is of course satisfying, since longer driving routes are seldom known in advance. However, this is probably dependent on which driving cycle that is used, and should also be tested for other cycles.

5.2 Future Work

The need for future work lies mainly within the area of optimization. The optimization algorithm developed could be extended by including a more accurate model, that is still convex. It would also be interesting to include an emission model in the objective function, to see how it changes the optimal power split. It is necessary to speed up the optimization algorithm if it is going to be used in a real environment. As it is implemented now, it is too slow, especially for long prediction horizons. Further, it would be interesting to see if an MPC strategy would change the resulting fuel consumption compared to the current

implementation of the optimization procedure.

The subject of drive shaft flexibility and regulation of drive shaft oscillations was unfortunately just shortly mentioned in this thesis. This is an area of great interest, that is rather undiscovered regarding hybrid electric vehicles.

References

- [1] AnnexVII-2000. Iea implementing agreement for hybrid and electric vehicle technologies and programmes. <http://www.ieahev.org/AnnexVII-2000.html>, August 2003.
- [2] K. Jonasson. *Analysing Hybrid Drive System Topologies*. PhD thesis, Department of Industrial Electrical Engineering, Lund University, Lund, Sweden, 2002.
- [3] Mattias Åsbogård Leo Laine, Jonas Hellgren. Specifications of a hybrid electric taxi. August 2002.
- [4] Lars Nielsen and Lars Eriksson. *Course Material Vehicular Systems*. Linköping Institute of technology, Vehicular Systems, ISY, 1 edition, 2002.
- [5] Gustaf Olsson and Mats Alaküla. *Elmaskinsystem*. IEA/LTH Lund, Lund, Sweden, 1 edition, 1997.
- [6] M. Pettersson. *Driveline Modeling and Control*. PhD thesis, Department of Electrical Engineering, Linköpings Universitet, Linköping, Sweden, 1997.
- [7] Philip T. Krein Robert A. Weinstock and Robert A. White. Optimal sizing and selection of hybrid electric vehicle components. pages 251–256, June 1993.
- [8] J. Seiler. *Betriebsstrategien für Hybridfahrzeuge mit Verbrennungsmotor unter der Berücksichtigung von Kraftstoffverbrauch und Schadstoffemissionen während der Warmlaufphase*. PhD thesis, Fakultät für Elektrotechnik und Informationstechnik, Technische Universität München, München, Germany, March 2000.
- [9] T.Sack V.H.Johnson, A.A. Pesaran. Center for transportation technologies and systems. <http://www.ctts.nrel.gov/BTM/pdfs/EVS17poster.pdf>, 2003.

Notation

Abbreviations

<i>HEV</i>	Hybrid Electric Vehicle
<i>ICE</i>	Internal Combustion Engine
<i>EM</i>	Electric Machine
<i>SOC</i>	State Of Charge
<i>CVT</i>	Continuously Variable Transmission
<i>NEDC</i>	New European Driving Cycle

Variables and parameters

λ	Air to fuel equivalence ratio
P_{ice}	Power produced by ICE
P_{em}	Power produced by EM
P_{prop}	Power needed to propell the vehicle
P_{brake}	Brake power
η_{ice}	ICE efficiency
η_{em}	EM efficiency
Q_{max}	Maximum battery charge
U_{em}	Battery voltage
k_{em}	EM magnetization
q_{HV}	Energy density
ψ	Fuel consumption (per second)
Ψ	Fuel consumption (total)
T	Torque
ω	Angular speed
v	Vehicle speed
i	Current
L_{em}	EM inner inductance
R_{em}	EM inner resistance

G	Gear ratio
I	Moment of inertia
m	Vehicle mass
r	Wheel radius
T_s	Sample time
\dot{m}_{ac}	Air mass flow into the cylinders
η_{vol}	Combustion engine volumetric efficiency
V_d	Displaced cylinder volume
N	Engine speed
n_r	Revolutions per cycle
R	Ideal gas constant
T_i	Intake manifold temperature
V_i	Intake manifold volume
\dot{m}_{at}	Air flow past the throttle
\dot{m}_{fc}	Fuel flow into the cylinders
\dot{m}_{fi}	Injected fuel flow
χ	Part of injected fuel that is deposited on the wall
τ_{fp}	Fuel evaporation time constant
m_{fp}	Fuel evaporated from the puddles
λ_{reg}	Correction term for air mass mixture regulation
AF_s	Stoichiometric air to fuel ratio
W_{ig}	Indicated gross work
W_p	Pumping work
W_f	Friction work
p_{em}	Exhaust manifold pressure
p_{im}	Intake manifold pressure
m_f	Fuel mass
q_{HV}	Fuel heating value
$\eta_{ig,c}$	Accounts for some energy losses in the engine
r_c	Compression ratio
γ	Specific heat ratio
$FMEP$	Friction mean effective pressure
ξ_{aux}	Load from auxiliary devices
B	Bore
mps	Mean piston speed
Π_{bl}	Boost layout
$BMEP$	Brake mean effective pressure
S_{ice}	Acceleration signal to ICE
S_{em}	Acceleration signal to EM
S_{brake}	Brake signal

Appendix A

Model parameters

Parameter	Value
EM Resistance (Ω)	0.7050
EM Inductance (H)	0.0091
EM Inertia ($kg \cdot m^2$)	0.01
Battery maximum load (Ah)	6.2
Maximum output voltage (V)	273.6
ICE Inertia ($kg \cdot m^2$)	0.1
Vehicle mass (kg)	1700
Wheel diameter (dm)	6

Appendix B

Simulink models

The models are implemented in Matlab/Simulink according to figures B.1 and B.2 on the following pages. The subsystems are not shown one by one, since the equations building them are already shown in chapter 2. Only the highest level of the Simulink scheme is shown so that the reader can see what the implementation environment looks like.

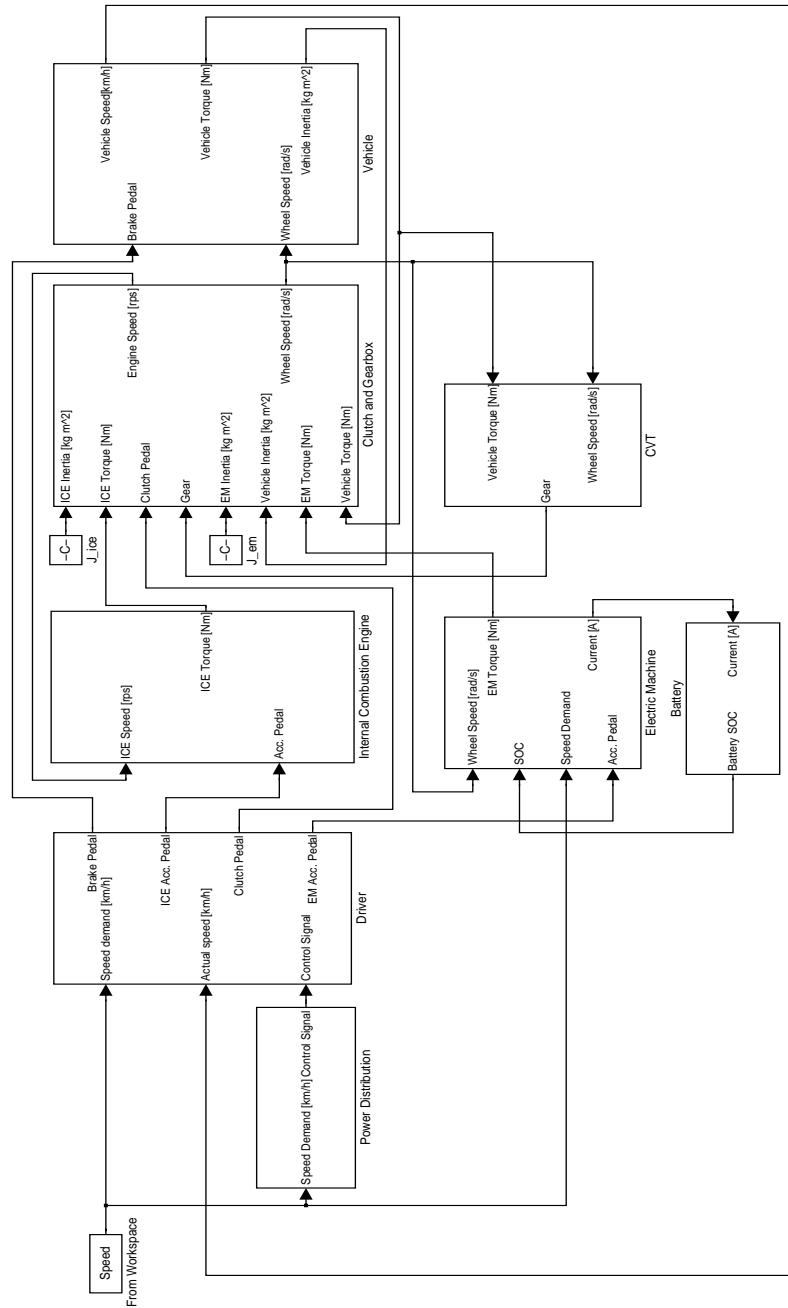


Figure B.1: Implementation of the parallel topology in Matlab/Simulink

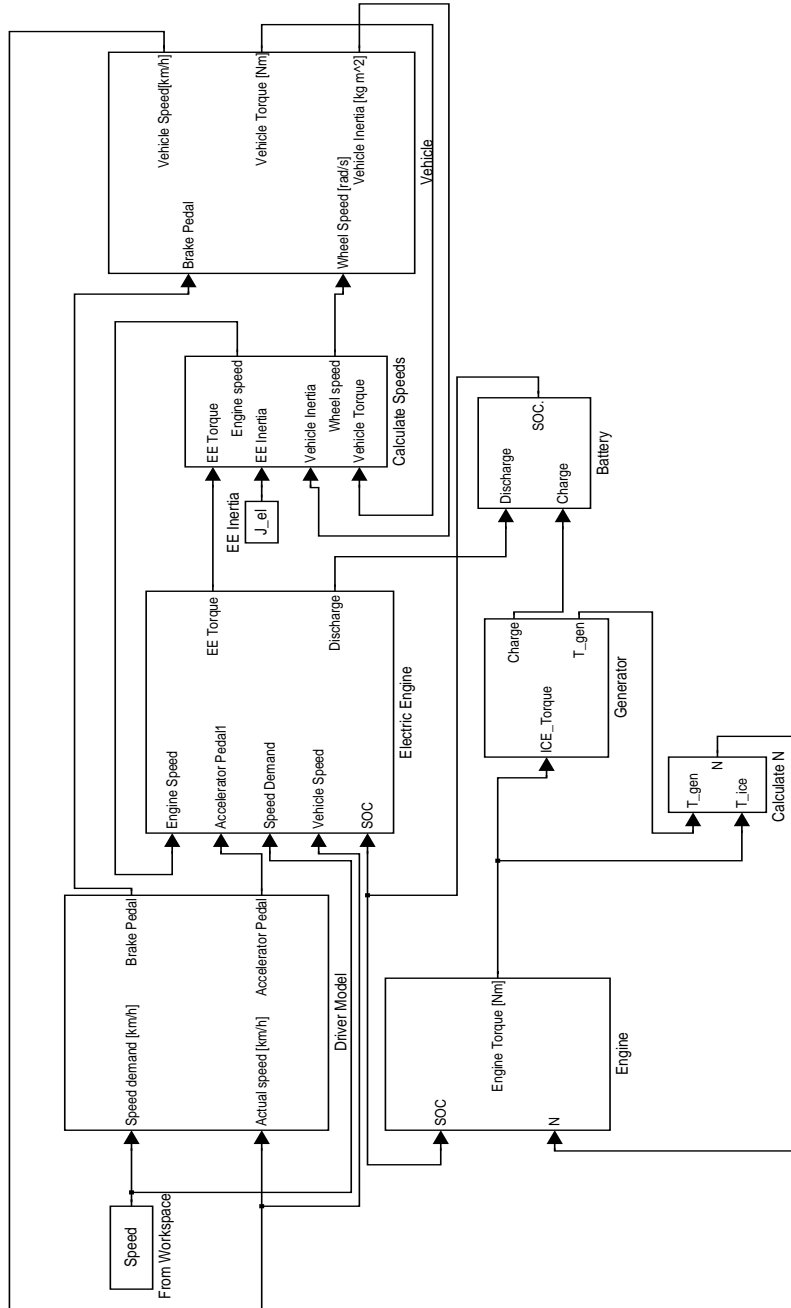


Figure B.2: Implementation of the series topology in Matlab/Simulink